Strain engineered barium strontium titanate for tunable thin film resonators

H. Khassaf,[1] N. Khakpash,[1] F. Sun,[2] N. M. Sbrockey,[3] G. S. Tompa,[3] T. S. Kalkur,[4] and S. P. Alpay[1,2,a)]
[1]*Department of Materials Science and Engineering and Institute of Materials Science, University of Connecticut, Storrs, Connecticut 06269, USA*
[2]*Department of Physics, University of Connecticut, Storrs, Connecticut 06269, USA*
[3]*Structured Materials Industries, Inc., Piscataway, New Jersey 08854, USA*
[4]*Department of Electrical and Computer Engineering, University of Colorado at Colorado Springs, Colorado Springs, Colorado 80918, USA*

(Received 23 April 2014; accepted 11 May 2014; published online 21 May 2014)

Piezoelectric properties of epitaxial (001) barium strontium titanate (BST) films are computed as functions of composition, misfit strain, and temperature using a non-linear thermodynamic model. Results show that through adjusting in-plane strains, a highly adaptive rhombohedral ferroelectric phase can be stabilized at room temperature with outstanding piezoelectric response exceeding those of lead based piezoceramics. Furthermore, by adjusting the composition and the in-plane misfit, an electrically tunable piezoelectric response can be obtained in the paraelectric state. These findings indicate that strain engineered BST films can be utilized in the development of electrically tunable and switchable surface and bulk acoustic wave resonators. © *2014 AIP Publishing LLC*. [http://dx.doi.org/10.1063/1.4879281]

Surface and bulk acoustic wave (SAW and BAW, respectively) resonators are important elements in several devices including remote controls, microprocessor clocks, mobile phones, and industrial controllers. The largest commercial application for acoustic resonators is for frequency selection in radio frequency (RF) telecommunication systems. Resonant frequency in SAW and BAW resonators depends on dimensions and properties of the material/materials systems of choice. Current technology SAW and BAW resonators employ a passive piezoelectric element such as aluminium nitride (AlN), and are neither switchable nor tunable. Such telecommunication systems use a bank of passive filters based on SAW or BAW resonators. Compound semiconductors such as GaAs or micro-electromechanical systems (MEMS) are then used as RF switches to select the appropriate fixed frequency filter. AlN exhibits strong chemical stability, excellent mechanical properties, and low dielectric losses combined with low leakage currents[1,2] and can be manufactured using recent developments in micromachining techniques.[3] On the other hand, it is a linear dielectric with a wurtzite crystal structure ($P6_3mc$) and has a weak piezoelectric response ($d_{33} \sim 5$ pm/V)[2] compared to ferroelectrics (FE) such as $(Pb,Zr)TiO_3$ (PZT) and its derivatives ($\sim$300 pm/V).[4,5]

Since the piezoelectric response of AlN is not electrically tunable, present AlN-based SAW and BAW resonators are fixed frequency devices.[6] Despite efforts to achieve electrical tuning in AlN-based resonators through implementation of sound guiding substrates and varying device dimensions, tunability in these systems is less than 1%.[7,8] Furthermore, current SAW and BAW devices must employ semiconductor or MEMS switches for frequency selection. As such, there exists a tremendous potential for the development of tunable and switchable thin film acoustic resonators. This would reduce the total parts count for RF products and would thus provide opportunities to manufacture smaller and cheaper devices. Piezoelectric tunability would enable frequency agile operation, eliminate filter banks as a costly and lossy source, and provide the possibility to get rid of the need for frequency trimming. For this purpose, FE materials have attracted attention as potential alternatives for AlN.[9] Because the electromechanical coupling depends on the spontaneous polarization, resonance in the FE state exhibits hysteresis.[3,10] However, since an appropriate electric field can distort central symmetry, emergence of piezoelectricity is possible in the paraelectric phase with the application of an external field. There are incipient FE or FE perovskites such as strontium titanate ($SrTiO_3$, STO)[3,11,12] and barium strontium titanate [$Ba_xSr_{1-x}TiO_3$, BST $x/(1-x)$][7,8,13–20] for which voltage induced electrostrictive resonance has been demonstrated in free-standing film or solidly mounted resonator (SMR)[7,13] device geometries.

In bulk, unconstrained BST, the phase transition temperature T_C can be varied by adjusting the relative amounts of Ba and Sr. T_C for pure barium titanate ($BaTiO_3$, BTO) is $\sim$120 °C, but by alloying systematically with STO, T_C can be lowered. For example, for BST 70/30 and 60/40, the cubic paraelectric to tetragonal FE transformations occur at $\sim$34 °C and $\sim$5 °C, respectively.[20] The ability to adjust T_C by controlling the composition is one of the most promising aspects of using BST in different types of resonators since piezoelectric response and its electric field tunability can be maximized near T_C. Misfit strain–temperature phase diagrams that were developed for monodomain epitaxial BST films[20,21] show that it is possible to induce FE phases with orthorhombic and rhombohedral symmetry that are not observed in bulk form.[22] In Fig. 1, we depict the prototypical perovskite BST crystal structure ($Pm3m$) in the bulk PE state and the FE states that can be induced through in-plane equi-biaxial misfit strains. The phases that appear in Fig. 2 are defined through the spontaneous polarization vector P_i ($i = 1,2,3$) such that: PE phase

a)Author to whom correspondence should be addressed. Electronic mail: p.alpay@ims.uconn.edu

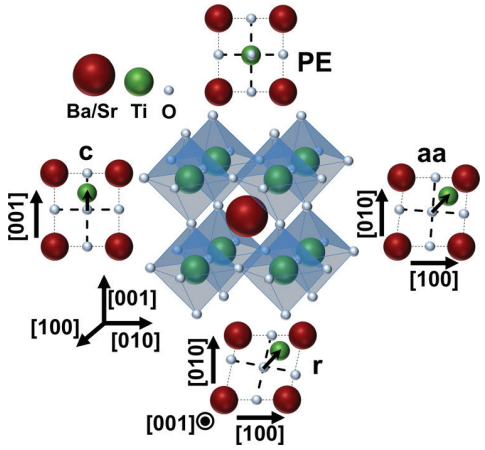

FIG. 1. At the center is the prototypical perovskite BST crystal structure where Ba/Sr atoms are surrounded by eight TiO_6 octahedra. Also shown are the possible strain induced phases. Polarization components in the tetragonal PE phase are $P_1 = P_2 = P_3 = 0$. The *c*-phase is tetragonal with $P_1 = P_2 = 0$, $P_3 \neq 0$. The *aa*-phase has an orthorhombic structure where $P_1 = P_2 \neq 0$ and $P_3 = 0$ and the *r*-phase is rhombohedral with $P_1 = P_2 \neq 0$ and $P_3 \neq 0$.

($P4mm$) with $P_1 = P_2 = P_3 = 0$, *c*–phase ($I\bar{4}3\,m$) with $P_1 = P_2 = 0$, $P_3 \neq 0$, *aa*–phase ($Amm2$) with $P_1 = P_2 \neq 0$ and $P_3 = 0$, and *r*–phase ($R3m$) with $P_1 = P_2 \neq 0$ and $P_3 \neq 0$.

In this study, we provide a theoretical analysis of piezoelectric response of epitaxial (001) BST films using a nonlinear thermodynamic model taking into account the appropriate electromechanical boundary conditions. We show that strain engineering is a powerful tool that could assist in the development of a new generation of acoustic resonators with extremely large piezoelectric coefficients which are also electrically tunable and/or switchable. Our results indicate that for certain BST compositions and small misfit strains ($-0.07 < u_m < 0.08\%$ and $-0.12 < u_m < 0.13\%$ for BST 80/20 and 90/10, respectively), the FE *r*-phase can be stabilized at room temperature (RT = 25 °C). The spontaneous polarization in this state can adapt itself to external stimuli through appropriate rotations and thus has very large piezoelectric response. BST films with lower Ba concentrations such as BST 60/40 remain paraelectric at RT for small misfit strains ($-0.04 < u_m < 0.04$). We demonstrate here that in this range, piezoelectric coefficients as high as ~300 pm/V can be realized with the application of external electric fields (400 kV/m). This behavior could be useful in certain telecommunication applications for which a paraelectric state may be preferred in order to avoid hysteresis losses associated with nucleation and growth of electrical domains.[14,23] The piezoelectric tunabilities of BST 60/40 in the FE *c*-phase region are 19% and 29% at 200 and 400 kV/m. These results suggest that tailoring the strain state in FE oxides could provide outstanding piezoelectric response compared to current simple oxide and nitride piezoelectric ceramics.

We employ here a Landau–Devonshire approach to compute the piezoelectric properties of heteroepitaxial BST films in different phase fields. A (001) monodomain epitaxial BST film on a thick (001) cubic substrate is considered. Taking into account the equi-biaxial in-plane polarization-free misfit strain $u_m = (a_S - a_F)/a_S$, where a_S and a_F are the lattice parameters of the substrate and the (pseudo-cubic) film, respectively, and an applied electrical field E_3//[001] perpendicular to the film–substrate interface, the (excess) free energy density of the film can be expressed as[20]

$$\begin{aligned}\Delta G = {} & a_1^*\left(P_1^2 + P_2^2\right) + a_3^* P_3^2 + a_{11}^*\left(P_1^4 + P_2^4\right) + a_{33}^* P_3^4 \\ & + a_{13}^*\left(P_1^2 P_3^2 + P_2^2 P_3^2\right) + a_{12}^* P_1^2 P_2^2 + a_{111}\left(P_1^6 + P_2^6 + P_3^6\right) \\ & + a_{111}\left[P_1^4\left(P_2^2 + P_3^2\right) + P_3^4\left(P_1^2 + P_2^2\right) + P_2^4\left(P_1^2 + P_3^2\right)\right] \\ & + a_{123} P_1^2 P_2^2 P_3^2 + \frac{u_m^2}{S_{11} + S_{12}} - E_3 P_3, \end{aligned} \tag{1}$$

with renormalized dielectric stiffness coefficients:

$$a_1^* = a_1 - u_m \frac{Q_{11} + Q_{12}}{S_{11} + S_{12}}, \tag{2a}$$

$$a_3^* = a_1 - u_m \frac{2Q_{11}}{S_{11} + S_{12}}, \tag{2b}$$

$$a_{11}^* = a_{11} + \frac{1}{2\left(S_{11}^2 - S_{12}^2\right)}\left[\left(Q_{11}^2 - Q_{12}^2\right)S_{11} - 2S_{11}Q_{12}S_{12}\right], \tag{2c}$$

$$a_{33}^* = a_{11}\frac{Q_{12}^2}{S_{11} + S_{12}}, \tag{2d}$$

$$\begin{aligned} a_{12}^* = {} & a_{12} - \frac{1}{\left(S_{11}^2 - S_{12}^2\right)} \\ & \times \left[\left(Q_{11}^2 + Q_{12}^2\right)S_{12} - 2S_{11}Q_{12}S_{11}\right] + \frac{Q_{44}^2}{2S_{44}}, \end{aligned} \tag{2e}$$

$$a_{13}^* = a_{12} + \frac{Q_{12}(Q_{11} + Q_{12})}{S_{11} + S_{12}}, \tag{2f}$$

where P_i ($i = 1,2,3$) are the components of the polarization vector, $a_1 = (T - T_C)/2\varepsilon_0 C$ is the dielectric stiffness, T_C and C are the Curie–Weiss temperature and constant of the bulk ferroelectric, ε_0 is the permittivity of free space, a_{ij} and a_{ijk} are higher order stiffness coefficients, Q_{ij} are the electrostrictive coefficients, and S_{ij} are the elastic compliances of the film in Voigt notation.

u_m–T phase diagrams are obtained by evaluating the equations of state $\partial\Delta G/\partial P_i = 0$ for $E_3 = 0$. The property coefficients used in the calculations are compiled from the literature.[20] In Fig. 2, we plot the stability regions of the FE and paraelectric phases for four compositions of BST (60/40, 70/30, 80/20, and 90/10) in temperature and misfit ranges of $-50 < T < 150$ °C and $-0.5 < u_m < 0.5\%$. Also shown in Fig. 2 is the variation of the total spontaneous polarization ($P = P_S = \sqrt{2P_{S,1}^2 + P_{S,3}^2}$) in each phase region. Regardless of the BST composition, the phase diagrams indicate that depending on T, there are two different sequences of phase transformations with increasing u_m from in-plane compressive to in-plane tensile misfits. At relatively higher temperatures, the *c*-phase which is more stable for in-plane compressive misfit strains transforms to the PE phase with increasing u_m at a critical misfit strain u_m^*. At $T = 100$ °C, for BST 60/40, 70/30, 80/20, and 90/10, u_m^* is −0.22%, −0.16%, −0.09%, and −0.01%, respectively. With increasing in-plane tensile strains, the *aa*-phase becomes more stable ($u_m > 0.20\%$ for BST 60/40 at $T = 100$ °C). Significant shifts in T_C and stabilization of metastable phases have been confirmed

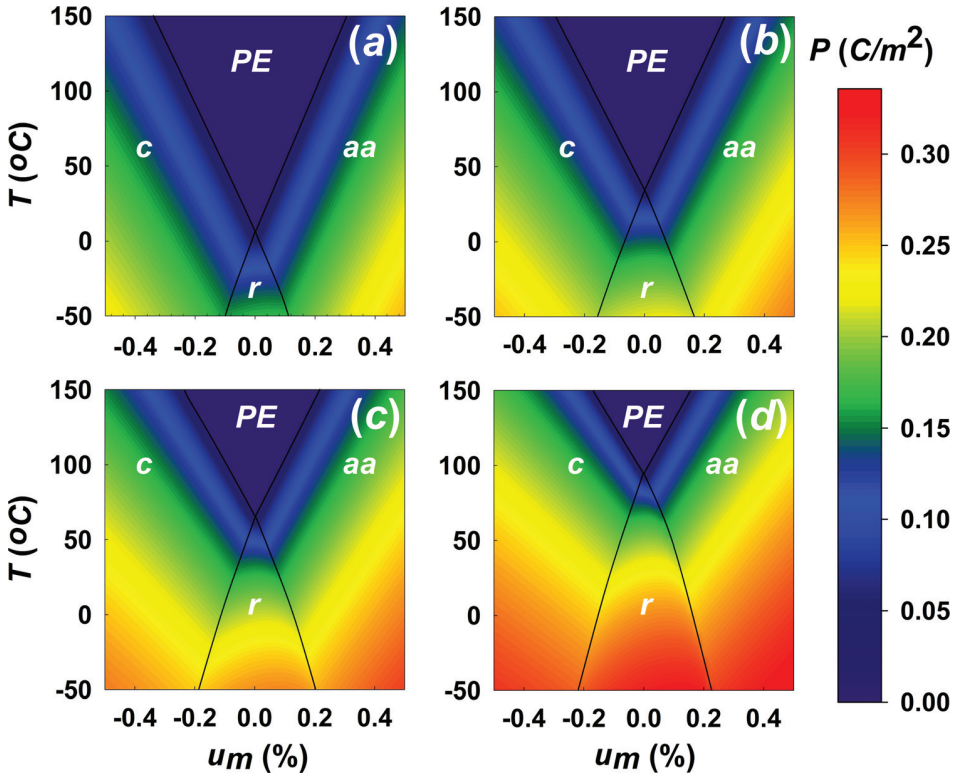

FIG. 2. Phase diagrams of various compositions [60/40, 70/30, 80/20, and 90/10 from (a) to (d), respectively] of monodomain epitaxial (001) BST films under compressive and tensile misfit strains on a thick (001) pseudo-cubic substrate in the temperature range of −50 °C–150 °C and variations of total polarization in the ferroelectric phase fields.

experimentally in similar epitaxial systems.[24,25] The *c*–PE and PE–*aa* transitions are of second-order due to the positive sign of the coefficients a^*_{11}, a^*_{12}, a^*_{13}, and a^*_{33}. This can also be verified by inspecting the variations in the polarization components in this field region. In Fig. 3(a), we plot as an example the change of the out-of-plane and in-plane spontaneous polarization of BST 60/40 at RT. Fig. 3(a) indicates that there are no "jumps" in P_3 and $P_1 = P_2$ at the critical misfit strains of −0.04% and 0.04% corresponding to the *c*–PE and PE–*aa* phase boundaries. For zero electric field, P_3 vanishes at the *c*–PE boundary while for $E_3 > 0$ the material is polarized in the [001] direction. In the case of in-plane polarization, however, application of electric field does not alter the material behavior since the out-of-plane electric field does not affect planar polarization. At relatively lower temperatures for the four compositions analyzed in this study, a *c*–*r*–*aa* phase transition sequence becomes possible. Both the *c*–*r* and *r*–*aa* phase transformations are of second order and this is confirmed in Fig. 4(a) where we plot the polarization components variation versus misfit strain for BST 80/20 at RT. We note that the stability region of the *r*-phase becomes narrower with decreasing Sr content. For BST 70/30 and BST 90/10, the phase fields of the *r*–phase are within $-0.018 < u_m < 0.02\%$ and $-0.112 < u_m < 0.129\%$.

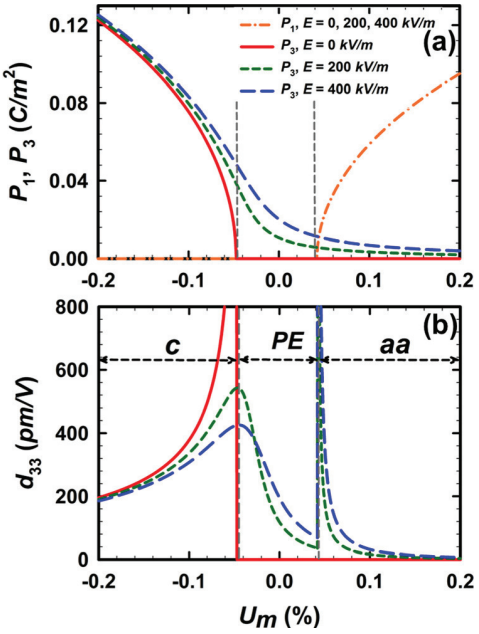

FIG. 3. (a) Variation of the in-plane and out-of-plane spontaneous polarization components as a function of misfit strain and (b) RT out-of-plane piezoelectric response (d_{33}) of (001) BST (60/40) for different electric fields. d_{33} in the PE region is zero for $E_3 = 0$. For $E_3 > 0$, there is a piezoelectric response in the PE region for misfit strains close to the *c*-PE transition.

The out–of–plane piezoelectric coefficients (d_{33}) for the four phases can be determined via

$$d_{33} = \begin{cases} 2\varepsilon_0\eta_{33}Q_{11}P_3 & PE \\ 2\varepsilon_0\eta_{33}Q_{11}P_3 & c-phase \\ 2\varepsilon_0(\eta_{33}Q_{11} + \eta_{23}Q_{12})P_3 & r-phase \\ 2\varepsilon_0(\eta_{11}Q_{11} + 2\eta_{12}Q_{12})P_3 & aa-phase, \end{cases} \quad (3)$$

where $\eta_{ij} = A_{ij}/\Delta$ are dielectric susceptibility coefficients, and A_{ij} and Δ are the cofactor and determinant of relative dielectric stiffness tensor.[26]

Fig. 3(b) shows the variation in d_{33} of (001) BST 60/40 as a function of u_m at RT for $E_3 = 0$, 200, and 400 kV/m. This particular composition is chosen as an illustration of piezoelectric properties in the *c*-PE-*aa* phase fields at RT. In both PE and *aa*-regions, there is no piezoelectric response for $E_3 = 0$. However, for $E_3 > 0$, excellent piezoelectric properties can be obtained. For instance, for $u_m = -0.02\%$, $E_3 = 200$ and 400 kV/m produce piezoelectric coefficients as high as ~250 and ~300 pm/V, respectively. Here, piezoelectricity emanates only due to the fact that the central symmetry of the crystal is broken with the application of an out-of-plane electric field. This is significant since it means that high values of d_{33} can be induced in the material system without hysteretic behavior—a fundamental characteristic of a FE material. To describe the piezoelectric behavior in *c-r-aa* phase fields, we chose (001) BST 80/20 at RT. Fig. 4(b) presents d_{33} for different electric field values. In the *r*-region, for misfit strains near the *c*–*r* phase transition, very high magnitudes of d_{33} values are predicted (e.g., $d_{33} = 1500$ pm/V for $u_m = -0.05\%$). The large piezoelectric properties in this region can be attributed to the ease by which the spontaneous polarization vector in the *r*-phase can adapt itself to external stimuli. The transition from the *c*-phase to the *r*-phase and then to the *aa*-phase occurs via a rotation of the spontaneous polarization from the [001] axis towards [110] direction. Because it is plotted in a log scale, in Fig. 4(b) the tunability of the piezoelectric coefficient in the *r*-region is not clearly displayed. For BST 80/20 and $u_m = 0.06\%$, the piezoelectric coefficient varies from 179 pm/V to 223 pm/V with a change in the applied field from 0 kV/m to 400 kV/m. In the *aa*-phase region, however, out-of-plane piezoelectric response can only be obtained with the application of E_3. While with zero electric field, piezoelectricity diminishes right before the *r-aa* transition. For $E_3 = 200$ and 400 kV/m, respectively, piezoelectric coefficients of 23 and 45 pm/V are achievable for $u_m = 0.12\%$.

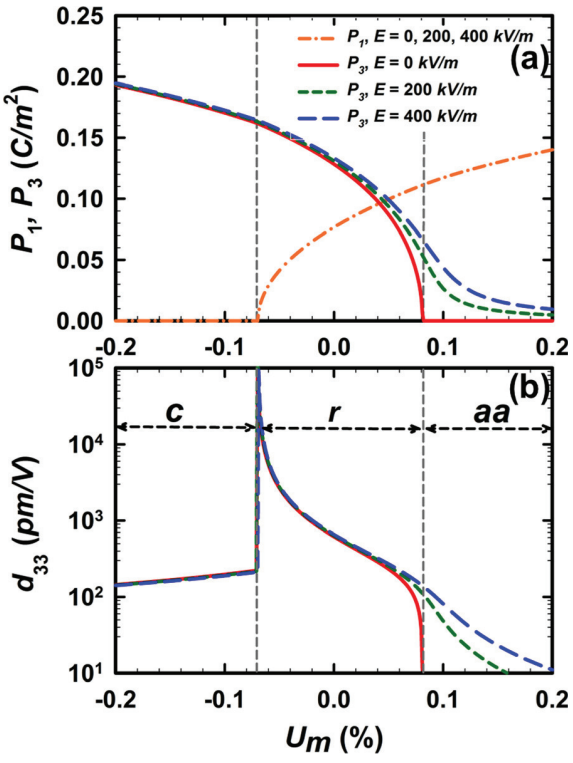

FIG. 4. (a) Variation of the in-plane and out-of-plane spontaneous polarization components as a function of misfit strain and (b) RT out-of-plane piezoelectric response (d_{33}) of (001) BST (80/20) for different electric fields.

It should also be noted that high lattice mismatches between BST and the substrate potentially could facilitate the process of strain relaxation that would hinder the accessibility of ferroelectric phases predicted by our calculations. In practice, there are several key factors that have impact on the interaction between the film and the substrate. It is shown that the stresses are almost completely relaxed with increasing film thickness through the formation of misfit strain dislocations at the film/substrate interface.[27] The higher the lattice mismatch between the film and the substrate, the smaller the critical thickness for relaxation through the generation of interfacial dislocations [Matthews–Blakeslee (MB) criteria].[28] The straightforward application of the MB criteria indicates that the critical thickness of misfit dislocation formation is relatively larger for lower processing temperatures due to the smaller thermal strain. Based on mechanisms by which interfacial dislocations are generated and the kinetics of the processes, experimental studies suggest that even for theoretical lattice mismatches larger than 7% for which the MB critical film thickness is typically of the range of 1–2 nm, complete relaxation does not occur until the film thickness reaches several hundred nanometers.[29] Therefore, depending on the deposition/processing/annealing temperatures and by the selection of substrate material, and film thickness, the level and sign of the misfit strain can be adjusted as to obtain optimum piezoelectric response.[20]

In this Letter, we have shown that how epitaxial strains can be used to obtain very high piezoelectric properties in a lead-free soft FE material. This study demonstrates that strain engineering of BST thin films provides an excellent opportunity to develop RF resonators that can be switched by using a low voltage control signal or can be frequency-tuned. Choice of substrate and application of appropriate electric fields could result in desired piezoelectric response both in paraelectric and FE phases. We also predict that electrically biased paraelectric BST exhibits outstanding piezoelectric behavior that provides the opportunity to deliver hysteresis free behavior. This would be beneficial in telecommunication technology to be established in tunable device configurations. The resulting components could reduce cost and improve performance for RF systems in a wide range of communications, radar, and wireless data applications.

We gratefully acknowledge financial support through Phase II STTR Contract No. W911NF-13-C-0029 from the Department of Defense, US Army Research Office. We also thank George A. Rossetti, Jr., for many useful discussions.

[1]R. B. Karabalin, M. H. Matheny, X. L. Feng, E. Defaÿ, G. Le-Rhun, C. Marcoux, S. Hentz, P. Andreucci, and M. L. Roukes, Appl. Phys. Lett. **95**, 103111 (2009).
[2]J. Hees, N. Heidrich, W. Pletschen, R. E. Sah, M. Wolfer, O. A. Williams, V. Lebedev, C. E. Nebel, and O. Ambacher, Nanotechnology **24**, 025601 (2013).
[3]N. M. Sbrockey, G. S. Tompa, T. S. Kalkur, J. Zhang, S. P. Alpay, and M. W. Cole, J. Vac. Sci. Technol. B **30**, 061202 (2012).

[4]Q. Guo, G. Z. Cao, and I. Y. Shen, J. Vib. Acoust. **135**, 011003 (2013).
[5]Z. Huang, Q. Zhang, S. Corkovic, R. Dorey, and R. W. Whatmore, IEEE Trans. Ultrason., Ferroelectr. Freq. Control **53**, 2287 (2006).
[6]A. N. Cleland, M. Pophristic, and I. Ferguson, Appl. Phys. Lett. **79**(13), 2070 (2001).
[7]J. Berge, A. Vorobiev, W. Steichen, and S. Gevorgian, IEEE Microwave Wireless Compon. Lett. **17**, 655 (2007).
[8]V. M. Mukhortov, S. V. Biryukov, Y. I. Golovko, G. Y. Karapet'yan, S. I. Masychev, and V. M. Mukhortov, Technol. Phys. Lett. **37**, 207 (2011).
[9]A. K. Tagantsev, V. O. Sherman, K. F. Astafiev, J. Venkatesh, and N. Setter, J. Electroceram. **11**(1–2), 5 (2003).
[10]A. Noeth, T. Yamada, V. O. Sherman, P. Muralt, A. K. Tagantsev, and N. Setter, J. Appl. Phys. **102**, 114110 (2007).
[11]K. Morito, Y. Iwazaki, T. Suzuki, and M. Fujimoto, J. Appl. Phys. **94**, 5199 (2003).
[12]G. N. Saddik, D. S. Boesch, S. Stemmer, and R. A. York, Appl. Phys. Lett. **91**, 043501 (2007).
[13]S. Tappe, U. Bottger, and R. Waser, Appl. Phys. Lett. **85**, 624 (2004).
[14]G. Subramanyam, M. W. Cole, N. X. Sun, T. S. Kalkur, N. M. Sbrockey, G. S. Tompa, X. Guo, C. Chen, S. P. Alpay, and G. A. Rossetti, Jr, J. Appl. Phys. **114**, 191301 (2013).
[15]N. K. Pervez, P. J. Hansen, and R. A. York, Appl. Phys. Lett. **85**, 4451 (2004).
[16]W. Chang, C. M. Gilmore, W. J. Kim, J. M. Pond, S. W. Kirchoefer, S. B. Qadri, D. B. Chirsey, and J. S. Horwitz, J. Appl. Phys. **87**, 3044 (2000).
[17]J. Im, O. Auciello, P. K. Baumann, S. K. Streiffer, D. Y. Kaufman, and A. R. Krauss, Appl. Phys. Lett. **76**, 625 (2000).
[18]C. L. Chen, J. Shen, S. Y. Chen, G. P. Luo, C. W. Chu, F. A. Miranda, F. W. Van Keuls, J. C. Jiang, E. I. Meletis, and H. Y. Chang, Appl. Phys. Lett. **78**, 652 (2001).
[19]S. Gevorgian, A. Vorobiev, and T. Lewin, J. Appl. Phys. **99**, 124112 (2006).
[20]Z. G. Ban and S. P. Alpay, J. Appl. Phys. **91**, 9288 (2002).
[21]L. Walizer, S. Lisenkov, and L. Bellaiche, Phys. Rev. B **73**, 144105 (2006).
[22]R. Dittmann, R. Plonka, E. Vasco, N. A. Pertsev, J. Q. He, C. L. Jia, S. Hoffmann-Eifert, and R. Waser, Appl. Phys. Lett. **83**, 5011 (2003).
[23]L. B. Kong, S. Li, T. S. Zhang, J. W. Zhai, F. Y. Chiang Boey, and J. Ma, Prog. Mater. Sci. **55**, 840 (2010).
[24]J. H. Haeni, P. Irvin, W. Chang, R. Uecker, P. Reiche, Y. L. Li, S. Choudhury, W. Tian, M. E. Hawley, B. Craigo, A. K. Tagantsev, X. Q. Pan, S. K. Streiffer, L. Q. Chen, S. W. Kirchoefer, J. Levy, and D. G. Schlom, Nature **430**(7001), 758 (2004).
[25]P.-E. Janolin, J. Mater. Sci. **44**(19), 5025 (2009).
[26]R. E. Newnham, *Properties of Materials: Anisotropy, Symmetry, Structure: Anisotropy, Symmetry, Structure* (Oxford University Press, 2004).
[27]J. S. Speck and W. Pompe, J. Appl. Phys. **76**, 466 (1994).
[28]J. W. Matthews and A. E. Blakeslee, J. Cryst. Growth **27**, 118 (1974).
[29]L. S. Peng, X. Xi, B. H. Moeckly, and S. P. Alpay, Appl. Phys. Lett. **83**, 4592 (2003).